Original Article

Association between resting myocardial work indices and stress myocardial perfusion in patients with angina and non-obstructive coronary artery disease

Ji-Chen Pan[1]^, Li-Juan Lyu[1]^, Quan-De Liu[1], Wei Yang[1]^, Xin-Hao Li[1]^, Ye-Ming Han[2], Jun-Yan Sun[2], Mei Dong[1], Peng-Fei Zhang[1]^, Mei Zhang[1]^

[1]Key Laboratory of Cardiovascular Remodeling and Function Research, Chinese Ministry of Education, Chinese National Health Commission and Chinese Academy of Medical Sciences, State and Shandong Province Joint Key Laboratory of Translational Cardiovascular Medicine, Department of Cardiology, Qilu Hospital, Cheeloo College of Medicine, Shandong University, Jinan, China; [2]Department of Radiology, Qilu Hospital, Cheeloo College of Medicine, Shandong University, Jinan, China

Contributions: (I) Conception and design: JC Pan, PF Zhang, M Zhang; (II) Administrative support: M Dong, M Zhang; (III) Provision of study materials or patients: PF Zhang, M Zhang; (IV) Collection and assembly of data: W Yang, XH Li, YM Han, JY Sun; (V) Data analysis and interpretation: JC Pan, LJ Lyu, QD Liu; (VI) Manuscript writing: All authors; (VII) Final approval of manuscript: All authors.

Correspondence to: Mei Zhang, MD, PhD. Key Laboratory of Cardiovascular Remodeling and Function Research, Chinese Ministry of Education, Chinese National Health Commission and Chinese Academy of Medical Sciences, State and Shandong Province Joint Key Laboratory of Translational Cardiovascular Medicine, Department of Cardiology, Qilu Hospital, Cheeloo College of Medicine, Shandong University, No.107 Wenhuaxi Road, Jinan 250012, China. Email: daixh@vip.sina.com.

Background: Myocardial work (MW) indices and longitudinal strain (LS) are sensitive markers of early left ventricular systolic dysfunction. Stress computed tomography myocardial perfusion imaging (CT-MPI) can assess early myocardial ischemia. The association between resting MW indices and stress myocardial perfusion remains unclear. This study compares resting MW indices with LS to assess stress myocardial perfusion in angina patients with non-obstructive coronary artery disease (CAD).

Methods: Eighty-four patients who underwent resting echocardiography, coronary computed tomography angiography, and stress CT-MPI were reviewed. Seventeen myocardial segments were divided into three regions according to the epicardial coronary arteries. Global indices included global longitudinal strain (GLS), global work index (GWI), global constructive work (GCW), global wasted work (GWW), and global work efficiency (GWE). Regional indices included regional longitudinal strain (RLS), regional work index (RWI), and regional work efficiency (RWE). Reduced global perfusion was defined as an average stress myocardial blood flow (MBF) <116 mL/100 mL/min for the whole heart. Reduced regional perfusion was defined as an average stress MBF <116 mL/100 mL/min for the coronary territories. No patients demonstrated obstructions in the epicardial coronary arteries (stenosis diameter <50%). The MW indices and LS were compared. Receiver operating characteristic curves were constructed and logistic regression analyses were used to investigate the predictors of reduced myocardial perfusion.

Results: Patients with reduced stress perfusion demonstrated reduced GLS, GWI, GCW, and GWE (P<0.05) and increased GWW (P<0.05). After adjustment for age and sex, GWE was still independently associated with reduced myocardial perfusion (odds ratio =0.386, 95% confidence interval: 0.214–0.697; P<0.05). Receiver operating characteristic curves reflected the good diagnostic ability of GWE and its superiority to GLS (area under the curve: 0.858 *vs.* 0.741). The optimal cutoff GWE value was 95%

^ ORCID: Ji-Chen Pan, 0000-0003-3569-6733; Li-Juan Lyu, 0000-0003-4592-6766; Wei Yang, 0000-0003-1307-3922; Xin-Hao Li, 0000-0003-1394-4265; Peng-Fei Zhang, 0000-0001-8048-425X; Mei Zhang, 0000-0001-6295-5070.

(sensitivity, 70%; specificity, 90%). Regions with lower stress perfusion showed lower RLS, RWI, and RWE (P<0.05). The optimal cutoff value of RWE for predicting reduced regional perfusion was 95%, with an area under the curve of 0.780, a sensitivity of 62%, and a specificity of 83%.

Conclusions: Resting MW indices perform well in assessing global and regional stress myocardial perfusion in angina patients with non-obstructive CAD, and GWE is superior to GLS in the global evaluations.

Keywords: Left ventricular systolic function; myocardial work indices; longitudinal strain; myocardial perfusion

Submitted Apr 06, 2022. Accepted for publication Mar 21, 2023. Published online May 09, 2023.
doi: 10.21037/qims-22-321
View this article at: https://dx.doi.org/10.21037/qims-22-321

Introduction

Noninvasive myocardial work (MW) indices recently emerge to non-invasively evaluate the left ventricular systolic function and have shown high diagnostic and prognostic value in patients with obstructive coronary artery disease (CAD) (1,2). However, angina mostly occurs during stress conditions, and many angina patients who are referred for coronary angiography or coronary computed tomography angiography (CCTA) demonstrate non-obstructive CAD (3-5).

A "one-stop" examination, including CCTA and dynamic stress computed tomography myocardial perfusion imaging (CT-MPI), has been proven to play a considerable role in diagnosing myocardial ischemia. With invasive coronary angiography >50% diameter stenosis or invasive fractional flow reserve <0.80 as the reference, the combination of CCTA and CT-MPI shows high specificity and sensitivity, compared to single photon emission computed tomography myocardial perfusion imaging (6). It can find out the structural and functional reasons for reduced stress myocardial blood flow (MBF) with high sensitivity, specificity, and accuracy, comparable to positron emission tomography myocardial perfusion imaging (7-12). Using such a strategy, patients with myocardial ischemia and non-obstructive CAD can be identified.

Myocardial ischemia results in hypoxia and worsens left ventricular systolic function. MW indices and longitudinal strain (LS) can non-invasively evaluate the left ventricular myocardial performance, demonstrating potential advantages over left ventricular ejection fraction (LVEF). Reducing resting global longitudinal strain (GLS) has been associated with stress-induced left ventricular wall motion abnormalities in patients with diabetes mellitus (13). Although diabetes mellitus is a risk factor for ischemia with non-obstructive coronary arteries, the fact that all patients develop diabetes mellitus may be a bias. It can't comprehensively represent the relationship between GLS and stress-induced ischemia in all patients with non-obstructive CAD. What's more, the MW indices, derived from the left ventricular pressure-strain loop, seem to show different changes under different cardiovascular pathological conditions (14), and the influence of stress-induced ischemia on resting global and regional MW indices remains unclear in patients with angina and non-obstructive CAD. This retrospective study aimed to explore the association between resting MW indices and stress myocardial perfusion in patients with angina and non-obstructive CAD and to compare the clinical values of resting LS and MW indices in assessing stress myocardial perfusion.

Methods

Study cohort

Patients in this retrospective study were collected from a tertiary centre. In total, the medical records of 84 consecutive patients (minimum age: 32 years; maximum age: 75 years) with typical or atypical angina (15) who successfully underwent resting echocardiography, CCTA, and dynamic stress CT-MPI from January 2020 to June 2021 were reviewed. The inclusion criteria were: (I) non-obstructive CAD, defined as lumen stenosis <50% and (II) good image quality. The exclusion criteria included: (I) a clear prior history of obstructive CAD or coronary revascularization; (II) a history of cardiomyopathy, severe valvular disease, and non-cardiogenic chest pain; (III) a history of cardiac arrhythmias; and (IV) poor image quality. The study was conducted in accordance with the Declaration of Helsinki (as revised in 2013). The study was approved by the institutional ethics board of Qilu Hospital and individual consent for this retrospective analysis was waived.

Acquisition of transthoracic echocardiographic indices

Transthoracic echocardiography was performed using a GE Vivid E95 ultrasound system (GE Vingmed Ultrasound, Horten, Norway) with an M5S 3.5 MHz transducer. Patients were scanned in the left lateral decubitus position. Blood pressure was measured before and after examination, and the mean value of systolic blood pressure was calculated. Standard two-dimensional images, consisting of three cardiac cycles triggered to the QRS complex, were saved in DICOM format for offline analysis. Poor image quality referred to images permitting visualization of <70% of the myocardial wall (16).

Left ventricular structural parameters were measured, including left ventricular internal diameter at end diastole, interventricular septal thickness, and left ventricular posterior wall thickness. Subsequently, LVEF was measured by the modified Simpson method.

The LS and MW indices were calculated by two doctors who did not know the results of CCTA and CT-MPI with GE EchoPAC software. At the end of systole, the mitral ring and the left ventricular apex were selected along the endocardium on apical four-, two- and three-chamber views. The automated algorithm tracked the myocardium and adjustments were made as needed. Subsequently, the time of aortic valve closure was automatically identified on the apical three-chamber view. Using the American Heart Association 17-segment model (17), a bull's-eye plot of LS was generated (*Figure 1A*,*1B*). The software calculated GLS from the weighted average of the LS of 17 segments. According to the orientation of the three epicardial coronary arteries, the 17 segments were classified into three regions, as previously described (18). The regional longitudinal strain (RLS) was determined from the average of the LS of the segments in each region. The GLS and RLS are expressed as absolute values.

The MW indices were calculated using a combination of left ventricular LS and a noninvasively estimated left ventricular pressure curve. With peak systolic pressure assumed to be equal to peak arterial pressure, the software constructed a noninvasive pressure curve adjusted according to the duration of the isovolumic phase and ejection phase defined by the timing of the aortic and mitral valve opening and closing events. The following indices were obtained: (I) global work index (GWI), area within the left ventricle pressure-strain loop; (II) global constructive work (GCW), an estimate of the work performed by the left ventricle segments, consisting of shortening during systole plus lengthening in isovolumic relaxation; (III) global wasted work (GWW), an estimate of the negative work of the left ventricle segments, consisting of myocardial lengthening during systole and shortening during isovolumic relaxation; (IV) global work efficiency (GWE), GCW divided by the sum of GCW and GWW.

Similarly, the bull's-eye plots of the work index (*Figure 1C*,*1D*) and work efficiency (*Figure 1E*,*1F*) were constructed, and the 17 segments were classified into three regions. The regional work index (RWI) and regional work efficiency (RWE) were determined from the average of indices and efficiencies of the segments in each region (18).

Acquisition of CCTA and CT-MPI images

All patients were told to refrain from taking heart-rate-controlling drugs for at least one day before the examination. A third-generation dual-source CT scanner (SOMATOM Force; Siemens Medical Solutions, Forchheim, Germany) was used and optimal image acquisition was performed at end-systole to minimize motion artifacts in the generated images to greatest extent possible. Based on calcium score scanning images, the scan range was determined from 1 cm below the carina to the diaphragm to cover the whole left ventricle.

After 3 minutes of continuous adenosine triphosphate or adenosine administration at a rate of 160 μg/kg/min, an iodinated contrast agent (100 mL; Ultravist, 370 mg iodine/mL, Bayer, Germany) was injected at a flow rate of 4.5–6.0 mL/s.

Dynamic stress CT-MPI started 4 seconds after initiating the iodinated contrast agent injection by triggering axial mode at 250 ms after the R wave (end systole). The entire left ventricle was imaged by the shuttle-mode acquisition technique. Depending on the heart rate, scans were performed every two or three cardiac cycles, completing 10–15 phases in 30 s. The following scan parameters were used: collimation =192*0.6 mm, gantry rotation time =250 ms, temporal resolution =66 ms, shuttle-mode z-axis coverage of 105 mm, tube voltage =70 kV, and automated tube current scaling. CARE kV and CARE dose 4D were used to reduce the radiation dose.

Five minutes after CT-MPI acquisition, CCTA scanning was initiated. The iodinated contrast agent was intravenously injected at a flow rate of 4–5 mL/s, followed by a 40 mL saline flush using a double-barrel high-pressure syringe. CCTA was performed using retrospective electrocardiography-gated sequential acquisition. Delay period images were collected 5 minutes later. With

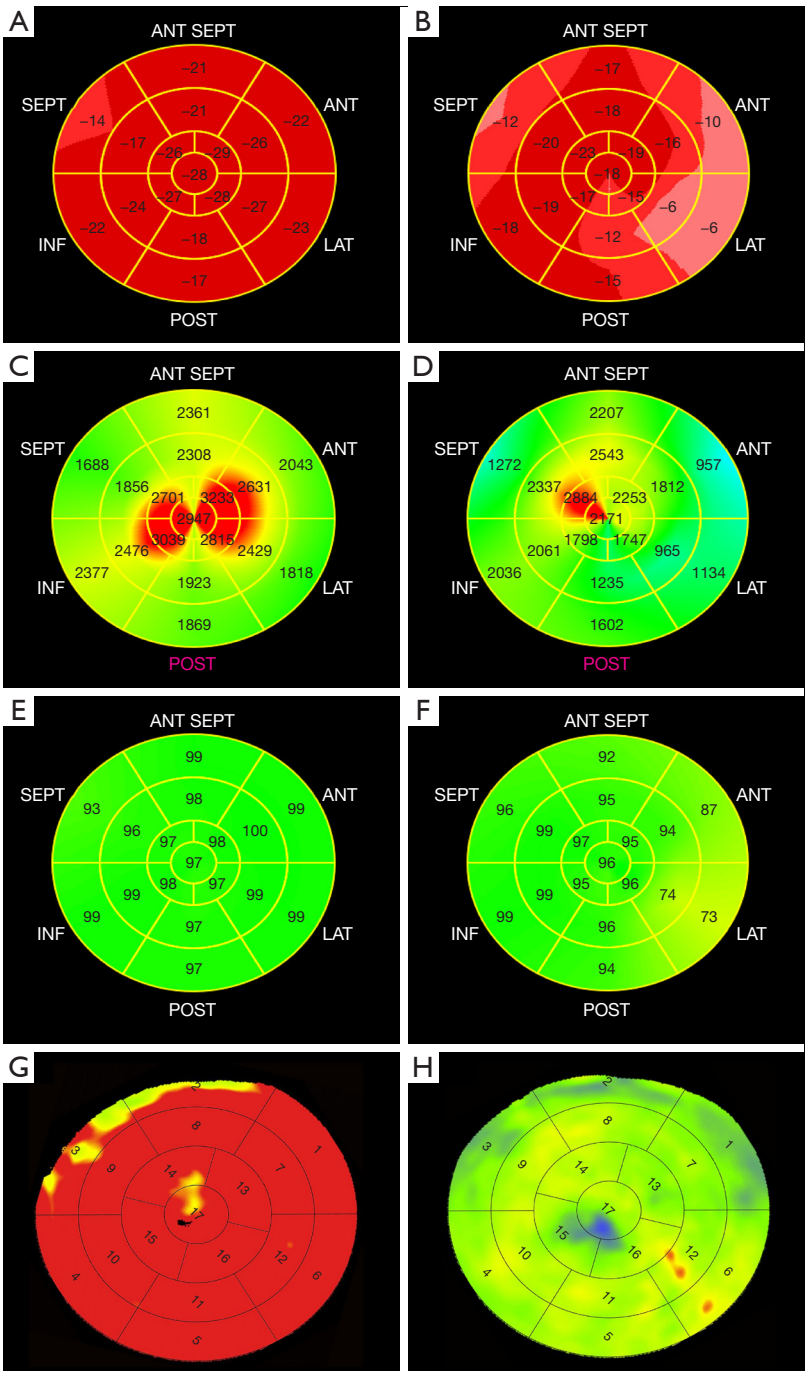

Figure 1 17-segment bull's-eye plots of echocardiographic mechanical indices and stress MBF. (A) Longitudinal strain bull's-eye plot from a subject with normal global stress myocardial perfusion. (B) Longitudinal strain bull's-eye plot from a subject with reduced global stress myocardial perfusion. (C) Work index bull's-eye plot from a subject with normal global stress myocardial perfusion. (D) Work index bull's-eye plot from a subject with reduced global stress myocardial perfusion. (E) Work efficiency bull's-eye plot from a subject with normal global stress myocardial perfusion. (F) Work efficiency bull's-eye plot from a subject with reduced global stress myocardial perfusion. (G) Stress MBF bull's-eye plot from a subject with normal global stress myocardial perfusion. (H) Stress MBF bull's-eye plot from a subject with reduced global stress myocardial perfusion. MBF, myocardial blood flow; ANT-SEPT, anterior interventricular septum; SEPT, interventricular septum; INF, inferior wall; POST, posterior wall; LAT, lateral wall; ANT, anterior wall.

the application of automated tube voltage and current modulation, the reference tube current was set to 320 mAs, and the reference tube voltage was set to 100 kV.

Myocardial perfusion software (VPCT body, Siemens Healthineers) built into the post-processing workstation (Syngo. Via VB10B; Siemens Healthineers) was used for the CT-MPI reconstruction. A dedicated kernel (b23f, Qr36) was used to reconstruct the CT-MPI images to reduce iodine beam-hardening artifacts. Motion correction was performed for all images. A circular region of interest was placed proximal and distal to the descending aorta to evaluate the time attenuation curve. A dedicated semiautomated parametric deconvolution algorithm based on a 2-compartment model of intravascular and extravascular space was used to derive MBF from the time attenuation curves. Short-axis and long-axis views of color-coded fused myocardium were reconstructed using cardiac functional models in Syngo.via VB10B.

Analysis of CCTA and CT-MPI images

CCTA and CT-MPI images were assessed by two experienced radiologists who were blinded to the echocardiographic results. As previously described (19), image quality was assessed with a 4-point scale (4 = poor, possible artifacts or poor image quality; 3 = moderate, likely artifacts, less likely perfusion defect; 2 = good, likely a defect, good image quality with no or minor artifacts; and 1 = excellent, no artifacts).

Stress MBF was presented as a 17-segment bull's-eye plot (*Figure 1G*,*1H*), and a region of interest was placed in each myocardial segment to quantify the MBF. The global MBF was calculated as the mean value of all 17 myocardial segments, and the regional MBF was calculated as the mean value of the myocardial segments in each region. For the analysis of CCTA images, the proximal and distal vessel segments without branches and stenosis were chosen as references. The shortest diameter of the lumen was measured at the site of stenosis.

$$\text{Percentage Stenosis} = 100\% - \frac{\text{lumen diameter at stenosis}}{\text{average of proximal and distal lumen diameter}} \quad [1]$$

Cut-off value of the MBF

In a previous study, our team assessed 51 healthy participants to calculate the cutoff stress MBF value (20). Assuming normally distributed data, the normal range was calculated as the mean ± SD*1.96 and the cutoff value was defined as the lower limit of the normal range. According to the Shapiro-Wilk test, stress MBF was normally distributed, and the MBF values were 164±24 mL/100 mL/min at both the patient and region levels. Therefore, the reference range of the MBF was 116-211 mL/100 mL/min. Reduced stress myocardial perfusion was defined as an MBF <116 mL/100 mL/min at both the patient and region levels. Patients and regions were divided into a normal perfusion group and a reduced perfusion group, respectively.

Effective radiation dose

The effective radiation dose was estimated from the dose-length product provided by the scanner and calculated according to the following formula: Effective radiation dose = dose-length product * κ [conversion coefficient κ_{Adult} =0.014 mSV/(mGy*cm)] (17).

Statistical analysis

Normality for continuous data was assessed by the Shapiro-Wilk test. Normally distributed variables are statistically described by the mean ± SD and were compared by Student's *t*-test. For non-normally distributed variables, the median (quartile spacing) is used for statistical description, and the Mann-Whitney U test was performed for comparisons between groups. Qualitative data are statistically expressed as numbers and percentages, and the chi-square test was used for comparisons between groups. Univariable and multivariable logistic regression analyses were performed to identify variables associated with reduced stress myocardial perfusion. A multivariable model including clinical data and mechanical parameters (P<0.1 in univariate logistic regression analysis) and receiver operating characteristic curves were constructed. The area under the curve (AUC) and the associated 95% confidence interval (CI) were calculated. A two-tailed P<0.05 was considered statistically significant. Statistical analyses were performed by using IBM SPSS Statistics (version 26.0) and MedCalc (version 15.8).

Twenty patients were randomly selected, subsequently, their GLS and global MW indices were measured by two double-blinded observers. Intraobserver variability was assessed from the same observer at two different time points. Interobserver variability was assessed by calculating the differences between measurements carried out for the same patient by two different observers. Intraobserver and interobserver variability were assessed using intraclass

Table 1 Clinical characteristics

Characteristics	Normal CT-MPI (n=61)	Reduced CT-MPI (n=23)	P
Male	22 (36%)	16 (70%)	0.006
Age (year)	55±10	59±8	0.087
BMI (kg/m^2)	24.97±3.39	25.57±3.31	0.470
BSA (m^2)	1.74±0.17	1.81±0.19	0.117
Systolic blood pressure (mmHg)	133±11	132±8	0.230
Diastolic blood pressure (mmHg)	79±9	82±10	0.254
Heart rates (bpm)	70±11	65±7	0.023
Smoking history	11 (18%)	7 (30%)	0.349
History of hypertension	18 (30%)	11 (48%)	0.115
History of DM	8 (13%)	6 (26%)	0.274
Family history of CAD	9 (15%)	7 (30%)	0.187
Cholesterol (mmol/L)	4.47±1.02	4.55±1.11	0.768
LDL-C (mmol/L)	2.71±0.85	2.70±1.00	0.987
HDL-C (mmol/L)	1.28±0.26	1.21±0.21	0.260
Triglyceride (mmol/L)	1.50 (0.69)	1.80 (1.20)	0.212

Data are presented as n (%), mean ± standard deviation, or median (quartile spacing). BMI, body mass index; BSA, body surface area; DM, diabetes mellitus; CAD, coronary artery disease; LDL-C, low density lipoprotein cholesterol; HDL-C, high density lipoprotein cholesterol; CT-MPI, computed tomography myocardial perfusion imaging.

correlation coefficients and Spearman's correlation coefficients.

Results

Clinical characteristics

One hundred and sixteen symptomatic patients without revascularization underwent successful echocardiography, CCTA, and dynamic stress CT-MPI within 1 week. Thirty-two patients were excluded: (I) 29 patients with obstructive CAD and (II) 3 patients with poor image quality. At the patient level, 61 (22 men, 55±10 years) patients were in the normal perfusion group, and 23 patients (16 men, age 59±8 years) were in the reduced perfusion group. The baseline parameters were shown in *Table 1*. The significant differences were observed only in the sex ratio and heart rates between the groups.

Effective radiation dose of CCTA and CT-MPI

The effective radiation doses of CCTA in the normal perfusion group and reduced perfusion group were 5.30 (4.14–6.80) mSv and 6.87 (4.98–8.03) mSv, respectively. Additionally, the effective radiation doses of dynamic stress CT-MPI in the normal perfusion group and reduced perfusion group were 4.37 (2.96–5.89) mSv and 4.49 (3.76–5.55) mSv, respectively.

Analysis of GLS and global MW indices

Compared to those in the normal perfusion group, GLS, GWI, GCW, and GWE were significantly lower (P<0.05) in the reduced perfusion group, while GWW was significantly higher (P<0.05) (*Table 2*).

In the univariable logistic regression analysis, resting GLS, GWI, GCW, GWW, and GWE were significantly associated with reduced global stress myocardial perfusion (all P<0.05). GCW and GWW were not included in the multivariable logistic analysis to avoid collinearity since the GWE incorporates GCW and GWW. Then, age [odds ratio (OR): 1.135, 95% CI: 1.008–1.277; P<0.05], GWI (OR: 0.994, 95% CI: 0.990–0.999; P<0.05) and GWE (OR: 0.386, 95% CI: 0.214–0.697; P<0.05) were found

Table 2 Resting echocardiographic parameters between the two groups

Parameters	Normal CT-MPI (n=61)	Reduced CT-MPI (n=23)	P
LVIDd (mm)	46 [5.5]	46 [6]	0.972
IVST (mm)	10 [2]	10 [2]	0.208
LVPWT (mm)	9 [2]	9 [2]	0.622
LVEF (%)	64±6	62±7	0.411
GLS (%)	22±2	19±2	<0.001
GWI (mmHg%)	2,346±368	2,006±280	<0.001
GCW (mmHg%)	2,661±425	2,339±306	<0.001
GWW (mmHg%)	57 [39]	107 [52]	<0.001
GWE (%)	97 [2]	95 [2]	<0.001

Data are presented as median [quartile spacing] or mean ± standard deviation. LVIDd, left ventricular internal diameter at end-diastole; IVST, interventricular septal thickness; LVPWT, left ventricular posterior wall thickness; LVEF, left ventricular ejection fraction; GLS, global longitudinal strain; GWI, global work index; GCW, global constructive work; GWW, global wasted work; GWE, global work efficiency; CT-MPI, computed tomography myocardial perfusion imaging.

to be independently associated with reduced global stress myocardial perfusion in the multivariable model (*Table 3*).

Receiver operating characteristic curve analysis was used to determine whether resting global MW indices and GLS could diagnose reduced global stress myocardial perfusion (*Figure 2A*). GWE had the highest AUC value among the analyzed variables (AUC: 0.858, P<0.05). The optimal cutoff GWE value for detecting reduced global stress myocardial perfusion was 95%, with a sensitivity of 70% and a specificity of 90% (*Table 4*).

Analysis of RLS and regional MW indices

A total of 252 regions were analyzed, consisting of 200 regions with normal perfusion and 52 regions with reduced perfusion. Compared to those in the normal perfusion group, the RLS, RWI, and RWE in the reduced perfusion group were significantly decreased (P<0.05) (*Table 5*). In univariable logistic regression analysis, RLS (OR: 0.726, 95% CI: 0.640–0.823; P<0.05), RWI (OR: 0.998, 95% CI: 0.997–0.999; P<0.05) and RWE (OR: 0.597, 95% CI: 0.503–0.709; P<0.05) were significantly associated with reduced regional stress perfusion. Subsequently, forward stepwise regression analyses showed that RLS (OR: 0.814, 95% CI: 0.710–0.934; P<0.05) and RWE (OR: 0.654, 95% CI: 0.546–0.784; P<0.05) were independently associated with reduced regional stress perfusion.

Receiver operating characteristic curve analysis demonstrated that RWE had the highest AUC among the analyzed variables (AUC: 0.780, P<0.05). The optimal cutoff RWE value for identifying regions with reduced stress perfusion was 95%, with a sensitivity of 62% and a specificity of 83% (*Table 6*, *Figure 2B*).

Intraobserver and interobserver variability

The GLS and global MW indices presented high intraobserver (r=0.964 for GLS, r=0.922 for GWI, r=0.947 for GCW, r=0.761 for GWW, r=0.818 for GWE; P<0.05) and interobserver (r=0.882 for GLS, r=0.904 for GWI, r=0.958 for GCW, r=0.812 for GWW, r=0.805 for GWE; P<0.05) repeatability. In addition, the intraclass correlation coefficients of the global MW indices and GLS were greater than 0.75 for intraobserver variability and interobserver variability respectively (*Table 7*).

Discussion

The results of this study show that resting MW indices can serve as an accurate tool for assessing stress myocardial perfusion. GWE shows a superior diagnostic capacity to GLS for angina patients with non-obstructive CAD.

Association between echocardiographic mechanical consequences and myocardial ischemia

MW indices have been reported to be significantly altered in patients with obstructive CAD and therefore have great

Table 3 Univariate and multivariate logistic analysis for reduced global stress myocardial perfusion

Parameters	Univariate logistic analysis		Multivariate logistic analysis	
	OR (95% CI)	P	OR (95% CI)	P
Sex	0.247 (0.088–0.692)	0.008	0.335 (0.061–1.830)	0.207
Age	1.049 (0.992–1.108)	0.091	1.135 (1.008–1.277)	0.036
BMI	1.056 (0.913–1.221)	0.466		
BSA	9.625 (0.556–166.7)	0.120		
Systolic blood pressure	0.974 (0.928–1.022)	0.285		
Diastolic blood pressure	1.031 (0.979–1.085)	0.252		
Heart rates	0.953 (0.906–1.002)	0.061	0.947 (0.864–1.037)	0.240
Smoking history	1.989 (0.660–5.988)	0.222		
History of hypertension	2.190 (0.817–5.869)	0.119		
History of DM	2.338 (0.711–7.695)	0.162		
Family history of CAD	2.528 (0.812–7.869)	0.109		
Cholesterol	1.073 (0.676–1.702)	0.765		
LDL-C	0.996 (0.579–1.712)	0.987		
HDL-C	0.305 (0.039–2.386)	0.258		
Triglyceride	1.652 (0.855–3.190)	0.135		
LVIDd	1.003 (0.915–1.100)	0.945		
IVST	1.232 (0.903–1.682)	0.188		
LVPWT	1.175 (0.857–1.611)	0.317		
LVEF	0.968 (0.895–1.046)	0.407		
GLS	0.619 (0.466–0.823)	0.001	1.435 (0.847–2.429)	0.179
GWI	0.996 (0.994–0.998)	<0.001	0.994 (0.990, 0.999)	0.012
GCW	0.997 (0.995–0.999)	0.003		
GWW	1.036 (1.018–1.054)	<0.001		
GWE	0.318 (0.186–0.544)	<0.001	0.386 (0.214–0.697)	0.002

BMI, body mass index; BSA, body surface area; DM, diabetes mellitus; CAD, coronary artery disease; LDL-C, low density lipoprotein cholesterol; HDL-C, high density lipoprotein cholesterol; LVIDd, left ventricular internal diameter at end-diastole; IVST, interventricular septal thickness; LVPWT, left ventricular posterior wall thickness; LVEF, left ventricular ejection fraction; GLS, global longitudinal strain; GWI, global work index; GCW, global constructive work; GWW, global wasted work; GWE, global work efficiency; OR, odds ratio; CI, confidence interval.

predictive potential (21-24); they have also been used as prognostic markers for patients with ST-segment elevation myocardial infarction (STEMI) (18,25-27). However, symptomatic patients with non-obstructive epicardial coronary arteries, in whom symptoms tend to occur when oxygen demand increases significantly, can also be encountered in clinical practice (28). Previous studies have demonstrated that patients with myocardial ischemia and non-obstructive CAD are also at high risk of developing cardiac dysfunction and major adverse cardiac events (29). Hence, investigating the association between resting MW indices and stress-induced ischemia in patients with non-obstructive CAD may help to identify early ischemia and prevent worse cardiovascular events.

In a study that included 47 patients with STEMI treated by successful percutaneous coronary intervention, Liu

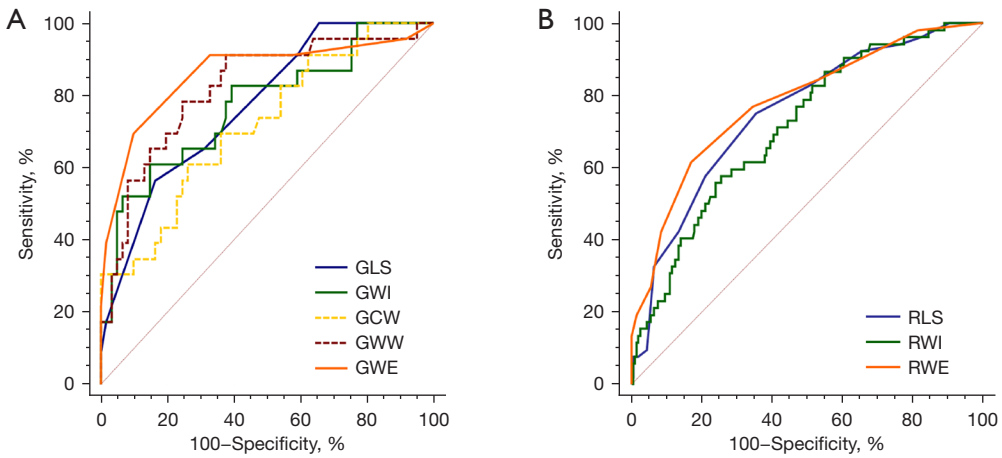

Figure 2 Receiver operating characteristic curve analysis of the mechanical indices for the prediction of reduced stress myocardial perfusion. (A) Receiver operating characteristic curve analysis of the global myocardial work indices and GLS for predicting reduced global stress myocardial perfusion. (B) Receiver operating characteristic curve analysis of the regional myocardial work indices and RLS for predicting reduced regional stress myocardial perfusion. GLS, global longitudinal strain; GWI, global work index; GCW, global constructive work; GWW, global wasted work; GWE, global work efficiency; RLS, regional longitudinal strain; RWI, regional work index; RWE, regional work efficiency.

Table 4 Receiver operating characteristic curve analysis for the detection of reduced global stress myocardial perfusion

Parameters	AUC	Cutoff value	Sensitivity, %	Specificity, %	PPV, %	NPV, %	P
GLS (%)	0.741	≤19	52	84	57	83	<0.001
GWI (mmHg%)	0.772	≤2,023	61	85	61	85	<0.001
GCW (mmHg%)	0.718	≤2,398	61	74	47	93	<0.001
GWW (mmHg%)	0.820	>76	78	75	55	90	<0.001
GWE (%)	0.858	≤95	70	90	73	89	<0.001

AUC, area under the curve; PPV, positive predictive value; NPV, negative predictive value; GLS, global longitudinal strain; GWI, global work index; GCW, global constructive work; GWW, global wasted work; GWE, global work efficiency.

Table 5 Resting regional myocardial work indices and RLS between the two groups

Parameters	Normal CT-MPI (n=200)	Reduced CT-MPI (n=52)	P
RLS (%)	22±3	19±3	<0.001
RWI (mmHg%)	2,269±431	1,958±344	<0.001
RWE (%)	97 [2]	95 [3]	<0.001

Data are presented as mean ± standard deviation or median [quartile spacing]. RLS, regional longitudinal strain; RWI, regional work index; RWE, regional work efficiency; CT-MPI, computed tomography myocardial perfusion imaging.

et al. found that resting global MW indices and GLS added additional value to the assessment of microvascular perfusion with myocardial contrast echocardiography (30). Although successful revascularization ensured no obstruction, the substantial effects of acute ischemia on the myocardium caused by preoperative acute coronary artery occlusion seemed inevitable to varying extents. In contrast, a reduced resting GLS has been proven to be associated with impaired

Table 6 Receiver operating characteristic curve analysis for the detection of reduced regional stress myocardial perfusion

Parameters	AUC	Cutoff value	Sensitivity, %	Specificity, %	PPV, %	NPV, %	P
RLS (%)	0.750	≤20	75	65	35	91	<0.001
RWI (mmHg%)	0.712	≤2,008	58	75	37	88	<0.001
RWE (%)	0.780	≤95	62	83	48	89	<0.001

AUC, area under the curve; PPV, positive predictive value; NPV, negative predictive value; RLS, regional longitudinal strain; RWI, regional work index; RWE, regional work efficiency.

Table 7 Inter- and intra-observer agreements of global myocardial work indices and GLS

Parameters	Interobserver		Intraobserver	
	ICCs	95% CI	ICCs	95% CI
GLS	0.880	0.721–0.951	0.948	0.875–0.979
GWI	0.906	0.780–0.962	0.913	0.797–0.964
GCW	0.944	0.865–0.977	0.954	0.888–0.982
GWW	0.878	0.674–0.953	0.780	0.530–0.906
GWE	0.817	0.600–0.923	0.848	0.659–0.937

GLS, global longitudinal strain; GWI, global work index; GCW, global constructive work; GWW, global wasted work; GWE, global work efficiency; ICCs, intraclass correlation coefficients; CI, confidence interval.

resting cardiac magnetic resonance myocardial perfusion (31,32). However, all patients in these studies were diagnosed with diabetes mellitus or hypertension, which might have resulted in selection bias. In our study, no significant difference in the prevalence of hypertension or diabetes mellitus was observed between the two groups. However, men seemed to be more likely to experience reduced stress myocardial perfusion, which was consistent with previous findings (33). First, men present with more traditional risk factors (34). Second, sex hormone differences may account for the higher proportion of men with reduced myocardial perfusion (35). Old age was another risk factor for reduced myocardial perfusion. Aging can result in increased arterial wall stiffness, medial thickening, and lumen enlargement, all of which may subsequently lead to endothelial dysfunction and subendocardial hypoperfusion over time. Furthermore, data on CCTA or invasive coronary angiography were not available for all patients in these studies. The influence of epicardial coronary lesions on strain could not be ignored because all patients were at high risk for obstructive CAD. Noticeably, early microvascular dysfunction, especially the functional phenotype, is not distinctive during resting conditions. Thus, in our study, CCTA and stress CT-MPI examinations were performed to screen out potential patients and avoid ignoring an early pathological state.

Our analysis of global and regional mechanical parameters in symptomatic patients without obstructive CAD and revascularization extends previous studies and confirms that abnormal resting echocardiographic mechanical consequences, markers of early systolic dysfunction, tend to occur in patients with stress-induced myocardial ischemia, indicating that they can be used as supplementary tests to screen patients for further stress myocardial perfusion imaging.

Pathological mechanism of changes in echocardiographic mechanical consequences

In our study, there were significant differences in global MW indices and GLS between the two patient groups, while there was no significant difference in LVEF. Myocardial ischemia initially affects the subendocardial myocardial fibers, whose motion is mainly longitudinal (21,36). Thus, LS and MW parameters could detect myocardial ischemia earlier and more accurately than LVEF, based on the fact that LVEF predominantly assesses radial function.

The significant alterations in resting MW indices and LS potentially reflect the pathological changes in the myocardium due to stress-induced myocardial ischemia.

Impaired stress myocardial perfusion without obstructive CAD may be a consequence of coronary microvascular dysfunction, presenting as microvascular sparsity, diastolic dysfunction in the arteriole, and decreased coronary flow reserve (37-39). The subendocardial myocardial fibers, which are responsible for longitudinal function, are most susceptible to early microvascular ischemia and vulnerable to replacement fibrosis (40,41). Repeated myocardial ischemia induced by exercise or agitation seems to be more common in clinical practice; frequent ischemia causes myocardial fibrosis, and there is a negative effect on myocardial contractility.

However, in multivariable logistic regression, GLS was not a risk factor for reduced stress myocardial perfusion, while GWI and GWE were. The causes may include the following. First, LS reflects only the peak systolic strain, not the relationship between myocardial contractility and oxygen consumption. The three prime determinants of oxygen consumption are heart rate, contractility, and afterload. MW indices overcome the afterload dependency of LS in estimating oxygen consumption and avoiding a misdiagnosis (42,43). Patients who demonstrated higher resting systolic blood pressure and lower GLS but normal stress myocardial perfusion could be identified accurately by global MW indices in this study. Second, MW indices are measured during the whole cardiac cycle and provide a perspective on the phase during which deformation occurs (44,45). The same strain peak in early or middle systole does not correspond to the same systolic function (22). Even shortening during isovolumetric relaxation is indicative of wasted work. Patients with reduced stress myocardial perfusion demonstrated a higher GWW in this study. Post-systolic shortening, which can be observed during isovolumetric relaxation, may be one of the reasons for such a situation, and it is considered a delayed contraction of ischemic myocardium (46,47). Similar to infarction, dyssynchrony has also been found in patients with myocardial ischemia (48). Additionally, contractile dysfunction may slow ventricular early relaxation due to the loss of elastic recoil. In contrast, GLS cannot distinguish such changes in one cardiac cycle. Left ventricular systolic and isovolumetric diastolic dysfunction is probably co-responsible for a reduced GWE.

Comparison between global MW indices and regional MW indices

GWE has been considered an effective diagnostic and prognostic marker in patients with STEMI (23,26). In our study, resting GWE was the most powerful parameter for diagnosing reduced stress global perfusion, and an optimal GWE cutoff value of 95% for reduced global stress myocardial perfusion was defined, with a sensitivity of 70% and a specificity of 90%. Moreover, after adjustment for age, sex, and other factors, GWE remained independently significant. This suggests that resting myocardial work indices may have potential clinical value in the diagnosis of stress-induced ischemia, avoiding the discomfort of pharmacological tests. Additionally, the global MW indices were highly consistent, in accordance with the results of previous studies (21,49), indicating excellent stability, which greatly enhanced the clinical value.

Interestingly, the ability of regional MW indices to diagnose reduced regional stress myocardial perfusion seemed to be slightly inferior. There may be a few reasons for this disparity. One myocardial region may present with reduced stress perfusion in patients with normal global stress myocardial perfusion. Nevertheless, during the resting state, the adequate blood supply from the collateral circulation could ensure the normal systolic function of the corresponding myocardial regions. This may have resulted in low sensitivity of the regional parameters. Microvascular dysfunction often leads to diffuse ischemia (50); therefore, patients with reduced global stress myocardial perfusion often have two or three myocardial regions with reduced stress perfusion, which may indicate severe and persistent ischemia. This may have more severe effects on longitudinal fibers; hence, global parameters are sensitive.

Limitations

There are still some limitations in the present study. First, this study has limitations inherent to its single-center and retrospective design. Further prospective studies with large-scale and multicenter samples are needed. In particular, the practical applicability of the regional MW indices needs to be examined in further studies, despite the differences found between regions with reduced and normal stress perfusion in this study. Second, although the resting MW indices can be used to assess stress myocardial perfusion, a longer follow-up will be needed to confirm the association between the resting MW indices and major advanced cardiovascular events. Third, although the GWE showed great diagnostic potential in identifying patients with reduced stress myocardial perfusion in this study, applying the parameter in patients with valvular lesions or peripheral vascular lesions is inappropriate because of a significant difference

between brachial systolic blood pressure and left ventricular pressure.

Conclusions

Resting MW indices perform well in assessing global and regional stress myocardial perfusion in angina patients with non-obstructive CAD, and GWE is superior to GLS in the global evaluations.

Acknowledgments

We thank American Journal Experts (AJE) for editing the English text of a draft of this manuscript.
Funding: The work was supported by the National Key Research and Development Program of China (No. 2016YFC1300302).

Footnote

Conflicts of Interest: All authors have completed the ICMJE uniform disclosure form (available at https://qims.amegroups.com/article/view/10.21037/qims-22-321/coif). The authors have no conflicts of interest to disclose.

Ethical Statement: The authors are accountable for all aspects of the work in ensuring that questions related to the accuracy or integrity of any part of the work are appropriately investigated and resolved. The study was conducted in accordance with the Declaration of Helsinki (as revised in 2013). The study was approved by the institutional ethics board of Qilu Hospital and individual consent for this retrospective analysis was waived.

References

1. Lin J, Wu W, Gao L, He J, Zhu Z, Pang K, Wang J, Liu M, Wang H. Global Myocardial Work Combined with Treadmill Exercise Stress to Detect Significant Coronary Artery Disease. J Am Soc Echocardiogr 2022;35:247-57.
2. Zhu H, Guo Y, Wang X, Yang C, Li Y, Meng X, Pei Z, Zhang R, Zhong Y, Wang F. Myocardial Work by Speckle Tracking Echocardiography Accurately Assesses Left Ventricular Function of Coronary Artery Disease Patients. Front Cardiovasc Med 2021;8:727389.
3. Thosar SS, Taqui S, Davidson B, Belcik T, Hodovan J, Rice SPM, Lindner JR. Resting coronary flow drives the daily pattern in coronary flow reserve in patients with chest pain without obstructive epicardial stenosis. Front Cardiovasc Med 2023;10:1057692.
4. Rahman H, Corcoran D, Aetesam-Ur-Rahman M, Hoole SP, Berry C, Perera D. Diagnosis of patients with angina and non-obstructive coronary disease in the catheter laboratory. Heart 2019;105:1536-42.
5. Tagliamonte E, Sperlongano S, Montuori C, Riegler L, Scarafile R, Carbone A, Forni A, Radmilovic J, Di Vilio A, Astarita R, Cice G, D'Andrea A. Coronary microvascular dysfunction affects left ventricular global longitudinal strain response to dipyridamole stress echocardiography: a pilot study. Heart Vessels 2023;38:470-7.
6. Narula J, Chandrashekhar Y, Ahmadi A, Abbara S, Berman DS, Blankstein R, Leipsic J, Newby D, Nicol ED, Nieman K, Shaw L, Villines TC, Williams M, Hecht HS. SCCT 2021 Expert Consensus Document on Coronary Computed Tomographic Angiography: A Report of the Society of Cardiovascular Computed Tomography. J Cardiovasc Comput Tomogr 2021;15:192-217.
7. Dewey M, Siebes M, Kachelrieß M, Kofoed KF, Maurovich-Horvat P, Nikolaou K, et al. Clinical quantitative cardiac imaging for the assessment of myocardial ischaemia. Nat Rev Cardiol 2020;17:427-50.
8. Celeng C, Leiner T, Maurovich-Horvat P, Merkely B, de Jong P, Dankbaar JW, van Es HW, Ghoshhajra BB, Hoffmann U, Takx RAP. Anatomical and Functional Computed Tomography for Diagnosing Hemodynamically Significant Coronary Artery Disease: A Meta-Analysis. JACC Cardiovasc Imaging 2019;12:1316-25.
9. Seitun S, Clemente A, De Lorenzi C, Benenati S, Chiappino D, Mantini C, Sakellarios AI, Cademartiri F, Bezante GP, Porto I. Cardiac CT perfusion and FFR(CTA): pathophysiological features in ischemic heart disease. Cardiovasc Diagn Ther 2020;10:1954-78.
10. Leo I, Nakou E, Artico J, Androulakis E, Wong J, Moon JC, Indolfi C, Bucciarelli-Ducci C. Strengths and weaknesses of alternative noninvasive imaging approaches for microvascular ischemia. J Nucl Cardiol 2023;30:227-38.

11. Tanabe Y, Kurata A, Matsuda T, Yoshida K, Baruah D, Kido T, Mochizuki T, Rajiah P. Computed tomographic evaluation of myocardial ischemia. Jpn J Radiol 2020;38:411-33.
12. Yang J, Dou G, He B, Jin Q, Chen Z, Jing J, Di Carli MF, Chen Y, Blankstein R. Stress Myocardial Blood Flow Ratio by Dynamic CT Perfusion Identifies Hemodynamically Significant CAD. JACC Cardiovasc Imaging 2020;13:966-76.
13. Albenque G, Rusinaru D, Bellaiche M, Di Lena C, Gabrion P, Delpierre Q, Malaquin D, Tribouilloy C, Bohbot Y. Resting Left Ventricular Global Longitudinal Strain to Identify Silent Myocardial Ischemia in Asymptomatic Patients with Diabetes Mellitus. J Am Soc Echocardiogr 2022;35:258-66.
14. Chan J, Edwards NFA, Khandheria BK, Shiino K, Sabapathy S, Anderson B, Chamberlain R, Scalia GM. A new approach to assess myocardial work by non-invasive left ventricular pressure-strain relations in hypertension and dilated cardiomyopathy. Eur Heart J Cardiovasc Imaging 2019;20:31-9.
15. Knuuti J, Wijns W, Saraste A, Capodanno D, Barbato E, Funck-Brentano C, et al. 2019 ESC Guidelines for the diagnosis and management of chronic coronary syndromes. Eur Heart J 2020;41:407-77.
16. Wilke L, Abellan Schneyder FE, Roskopf M, Jenke AC, Heusch A, Hensel KO. Speckle tracking stress echocardiography in children: interobserver and intraobserver reproducibility and the impact of echocardiographic image quality. Sci Rep 2018;8:9185.
17. Yi Y, Xu C, Wu W, Shen ZJ, Lee W, Yun CH, Lu B, Zhang JY, Jin ZY, Wang YN. Low-dose CT perfusion with combined use of CTP and CTP-derived coronary CT angiography at 70 kVp: validation with invasive fractional flow reserve. Eur Radiol 2021;31:1119-29.
18. Lustosa RP, Fortuni F, van der Bijl P, Goedemans L, El Mahdiui M, Montero-Cabezas JM, Kostyukevich MV, Ajmone Marsan N, Bax JJ, Delgado V, Knuuti J. Left ventricular myocardial work in the culprit vessel territory and impact on left ventricular remodelling in patients with ST-segment elevation myocardial infarction after primary percutaneous coronary intervention. Eur Heart J Cardiovasc Imaging 2021;22:339-47.
19. Feuchtner G, Goetti R, Plass A, Wieser M, Scheffel H, Wyss C, Stolzmann P, Donati O, Schnabl J, Falk V, Alkadhi H, Leschka S, Cury RC. Adenosine stress high-pitch 128-slice dual-source myocardial computed tomography perfusion for imaging of reversible myocardial ischemia: comparison with magnetic resonance imaging. Circ Cardiovasc Imaging 2011;4:540-9.
20. Lyu L, Pan J, Li D, Li X, Yang W, Dong M, Guo C, Lin P, Han Y, Liang Y, Sun J, Yu D, Zhang P, Zhang M. Knowledge of Hyperemic Myocardial Blood Flow in Healthy Subjects Helps Identify Myocardial Ischemia in Patients With Coronary Artery Disease. Front Cardiovasc Med 2022;9:817911.
21. Edwards NFA, Scalia GM, Shiino K, Sabapathy S, Anderson B, Chamberlain R, Khandheria BK, Chan J. Global Myocardial Work Is Superior to Global Longitudinal Strain to Predict Significant Coronary Artery Disease in Patients With Normal Left Ventricular Function and Wall Motion. J Am Soc Echocardiogr 2019;32:947-57.
22. Sabatino J, De Rosa S, Leo I, Strangio A, Spaccarotella C, Polimeni A, Sorrentino S, Di Salvo G, Indolfi C. Prediction of Significant Coronary Artery Disease Through Advanced Echocardiography: Role of Non-invasive Myocardial Work. Front Cardiovasc Med 2021;8:719603.
23. El Mahdiui M, van der Bijl P, Abou R, Ajmone Marsan N, Delgado V, Bax JJ. Global Left Ventricular Myocardial Work Efficiency in Healthy Individuals and Patients with Cardiovascular Disease. J Am Soc Echocardiogr 2019;32:1120-7.
24. Liu Y, Cui C, Li Y, Wang Y, Hu Y, Bai M, Huang D, Zheng Q, Liu L. Predictive value of the echocardiographic noninvasive myocardial work index for left ventricular reverse remodeling in patients with multivessel coronary artery disease after percutaneous coronary intervention. Quant Imaging Med Surg 2022;12:3725-37.
25. Butcher SC, Lustosa RP, Abou R, Marsan NA, Bax JJ, Delgado V. Prognostic implications of left ventricular myocardial work index in patients with ST-segment elevation myocardial infarction and reduced left ventricular ejection fraction. Eur Heart J Cardiovasc Imaging 2022;23:699-707.
26. Lustosa RP, Butcher SC, van der Bijl P, El Mahdiui M, Montero-Cabezas JM, Kostyukevich MV, Rocha De Lorenzo A, Knuuti J, Ajmone Marsan N, Bax JJ, Delgado V. Global Left Ventricular Myocardial Work Efficiency and Long-Term Prognosis in Patients After ST-Segment-Elevation Myocardial Infarction. Circ Cardiovasc Imaging 2021;14:e012072.
27. Mahdiui ME, van der Bijl P, Abou R, de Paula Lustosa R, van der Geest R, Ajmone Marsan N, Delgado V, Bax JJ. Myocardial Work, an Echocardiographic Measure of Post Myocardial Infarct Scar on Contrast-Enhanced Cardiac

Magnetic Resonance. Am J Cardiol 2021;151:1-9.
28. Woudstra J, Vink CEM, Schipaanboord DJM, Eringa EC, den Ruijter HM, Feenstra RGT, Boerhout CKM, Beijk MAM, de Waard GA, Ong P, Seitz A, Sechtem U, Piek JJ, van de Hoef TP, Appelman Y. Meta-analysis and systematic review of coronary vasospasm in ANOCA patients: Prevalence, clinical features and prognosis. Front Cardiovasc Med 2023;10:1129159.
29. Mehta PK, Quesada O, Al-Badri A, Fleg JL, Volgman AS, Pepine CJ, Merz CNB, Shaw LJ. Ischemia and no obstructive coronary arteries in patients with stable ischemic heart disease. Int J Cardiol 2022;348:1-8.
30. Liu R, Liu Y, Fei W, Wu Y, Lai Y. The role of myocardial work in evaluating coronary microcirculation of STEMI patients after percutaneous coronary intervention. Echocardiography 2021;38:2060-8.
31. Liu X, Yang ZG, Gao Y, Xie LJ, Jiang L, Hu BY, Diao KY, Shi K, Xu HY, Shen MT, Ren Y, Guo YK. Left ventricular subclinical myocardial dysfunction in uncomplicated type 2 diabetes mellitus is associated with impaired myocardial perfusion: a contrast-enhanced cardiovascular magnetic resonance study. Cardiovasc Diabetol 2018;17:139.
32. Li XM, Jiang L, Guo YK, Ren Y, Han PL, Peng LQ, Shi R, Yan WF, Yang ZG. The additive effects of type 2 diabetes mellitus on left ventricular deformation and myocardial perfusion in essential hypertension: a 3.0 T cardiac magnetic resonance study. Cardiovasc Diabetol 2020;19:161.
33. Gyllenhammar T, Carlsson M, Jögi J, Arheden H, Engblom H. Myocardial perfusion by CMR coronary sinus flow shows sex differences and lowered perfusion at stress in patients with suspected microvascular angina. Clin Physiol Funct Imaging 2022;42:208-19.
34. Kwan AC, Wei J, Ouyang D, Ebinger JE, Merz CNB, Berman D, Cheng S. Sex differences in contributors to coronary microvascular dysfunction. Front Cardiovasc Med 2023;10:1085914.
35. Haider A, Bengs S, Portmann A, Rossi A, Ahmed H, Etter D, et al. Role of sex hormones in modulating myocardial perfusion and coronary flow reserve. Eur J Nucl Med Mol Imaging 2022;49:2209-18.
36. Dahlslett T, Karlsen S, Grenne B, Eek C, Sjøli B, Skulstad H, Smiseth OA, Edvardsen T, Brunvand H. Early assessment of strain echocardiography can accurately exclude significant coronary artery stenosis in suspected non-ST-segment elevation acute coronary syndrome. J Am Soc Echocardiogr 2014;27:512-9.
37. Lam JH, Quah JX, Davies T, Boos CJ, Nel K, Anstey CM, Stanton T, Greaves K. Relationship between coronary microvascular dysfunction and left ventricular diastolic function in patients with chest pain and unobstructed coronary arteries. Echocardiography 2020;37:1199-204.
38. Taqueti VR, Shah AM, Everett BM, Pradhan AD, Piazza G, Bibbo C, et al. Coronary Flow Reserve, Inflammation, and Myocardial Strain: The CIRT-CFR Trial. JACC Basic Transl Sci 2022;8:141-51.
39. Carabelli A, Canu M, de Fondaumière M, Debiossat M, Leenhardt J, Broisat A, Ghezzi C, Vanzetto G, Fagret D, Barone-Rochette G, Riou LM. Noninvasive assessment of coronary microvascular dysfunction using SPECT myocardial perfusion imaging and myocardial perfusion entropy quantification in a rodent model of type 2 diabetes. Eur J Nucl Med Mol Imaging 2022;49:809-20.
40. Gao Y, Ren Y, Guo YK, Liu X, Xie LJ, Jiang L, Shen MT, Deng MY, Yang ZG. Metabolic syndrome and myocardium steatosis in subclinical type 2 diabetes mellitus: a (1)H-magnetic resonance spectroscopy study. Cardiovasc Diabetol 2020;19:70.
41. Mehrotra P, Jansen K, Flynn AW, Tan TC, Elmariah S, Picard MH, Hung J. Differential left ventricular remodelling and longitudinal function distinguishes low flow from normal-flow preserved ejection fraction low-gradient severe aortic stenosis. Eur Heart J 2013;34:1906-14.
42. Edwards NFA, Scalia GM, Sabapathy S, Anderson B, Chamberlain R, Khandheria BK, Chan J. Resting global myocardial work can improve interpretation of exercise stress echocardiography. Int J Cardiovasc Imaging 2021;37:2409-17.
43. Wang RR, Tian T, Li SQ, Leng XP, Tian JW. Assessment of Left Ventricular Global Myocardial Work in Patients With Different Degrees of Coronary Artery Stenosis by Pressure-Strain Loops Analysis. Ultrasound Med Biol 2021;47:33-42.
44. Przewlocka-Kosmala M, Marwick TH, Mysiak A, Kosowski W, Kosmala W. Usefulness of myocardial work measurement in the assessment of left ventricular systolic reserve response to spironolactone in heart failure with preserved ejection fraction. Eur Heart J Cardiovasc Imaging 2019;20:1138-46.
45. Zhu M, Wang Y, Cheng Y, Su Y, Chen H, Shu X. The value of non-invasive myocardial work indices derived from left ventricular pressure-strain loops in predicting the response to cardiac resynchronization therapy. Quant Imaging Med Surg 2021;11:1406-20.
46. Giridharan S, Karthikeyan S, Aashish A, Ganesh BA,

Prasath PA, Usha P. Two-dimensional speckle tracking echocardiography derived post systolic shortening in patients with unstable angina and normal left ventricular systolic function. Anatol J Cardiol 2021;25:880-6.
47. Lu S, Hu X, Zhang J, Zhu Y, Zhou W, Liu Y, Deng Y. Post-systolic shortening is superior to global longitudinal strain in predicting adverse events in patients with stable coronary artery disease and preserved systolic function. Insights Imaging 2022;13:35.
48. Hämäläinen H, Corovai A, Laitinen J, Laitinen TM, Hedman M, Hedman A, Kivelä A, Laitinen TP. Myocardial ischemia and previous infarction contribute to left ventricular dyssynchrony in patients with coronary artery disease. J Nucl Cardiol 2021;28:3010-20.
49. Ke QQ, Xu HB, Bai J, Xiong L, Li MM. Evaluation of global and regional left ventricular myocardial work by echocardiography in patients with chronic kidney disease. Echocardiography 2020;37:1784-91.
50. Kaski JC, Crea F, Gersh BJ, Camici PG. Reappraisal of Ischemic Heart Disease. Circulation 2018;138:1463-80.

Cite this article as: Pan JC, Lyu LJ, Liu QD, Yang W, Li XH, Han YM, Sun JY, Dong M, Zhang PF, Zhang M. Association between resting myocardial work indices and stress myocardial perfusion in patients with angina and non-obstructive coronary artery disease. Quant Imaging Med Surg 2023;13(7):4563-4577. doi: 10.21037/qims-22-321

